# Resolution of Benzophenone Delayed Fluorescence and Phosphorescence with Compensation for Thermal Broadening

**Andrzej M. Turek,*,† Govindarajan Krishnamoorthy, Kathleen Phipps, and Jack Saltiel***

*Department of Chemistry, The Florida State University, Tallahassee, Florida 32306-4390*

*Received: January 8, 2002*

Principal component analysis with self-modeling based on the van't Hoff equation constraint was applied to a set of benzophenone luminescence spectra from degassed carbon tetrachloride solutions in the 14.7−88.5 °C range. This analysis differs from an earlier treatment in that it was preceded by compensation of the spectra for differential broadening with increasing *T*. A set of Gaussians was derived as previously described [Saltiel, J.; Sears, D. F., Jr.; Turek, A. M. *J. Phys. Chem. A* **2001**, *105*, 7569−7578] that, on convolution with the spectrum for each corresponding *T*, creates a uniformly broadened spectral set. Significant improvements in the accuracy of the resolved delayed fluorescence and phosphorescence spectra lead to a reliable comparison between prompt and delayed fluorescence spectra that confirms the conclusion that the short $S_1$ lifetime prevents full relaxation of emitting benzophenone singlets. The enthalpy difference for the $T_1/S_1$ equilibrium, $5.50 \pm 0.06$ kcal/mol, agrees with the energy difference between the 0−0 bands of the resolved spectra, and the entropy difference is predicted nearly exactly by the difference in multiplicity between the two states ($-R \ln 3 = -2.18$ eu).

## Introduction

Due to small $S_1-T_1$ energy gaps, the luminescence of benzophenone in the vapor phase,[1] in degassed solutions,[2] and in rigid media[3] is composed of phosphorescence (P) from the $T_1$ state and delayed fluorescence (DF) from the thermally accessible $S_1$ state. Derivation of pure component P and DF spectra, based on principal component analysis with self-modeling (PCA-SM) treatment of a spectrothermal matrix of benzophenone luminescence spectra obtained from a degassed $CCl_4$ solution in the −2.4 to +85.2 °C range, led to the conclusion that the DF spectrum differs significantly from the prompt fluorescence spectrum (PF).[4] This interesting result suggested that PF originates, at least in part, from vibrationally hot $S_1$ states because vibrational relaxation in $S_1$ is not sufficiently fast to compete with the rate constant for $S_1 \rightarrow T_1$ intersystem crossing, $1.0 \times 10^{11}$ $s^{-1}$. It appeared to confirm the conclusion reached earlier by Hochstrasser and co-workers on the basis of differences in time-resolved $T_n \leftarrow T_1$ absorption spectra.[5] However, since the PCA-SM resolution neglected nonlinear temperature-induced changes in the spectra due to thermal broadening, the accuracy of the derived DF spectrum is in question and so is its comparison with the PF spectrum.

In this paper we achieve a much more reliable resolution of DF and P spectra by applying our recently developed method for broadening compensation in spectrothermal matrices[6] to a new set of benzophenone emission spectra. More reasonable thermodynamic parameters for $S_1/T_1$ equilibration are derived.

## Experimental Section

**Materials.** Benzophenone (Fischer, certified reagent) was recrystallized twice from hexane and then triply sublimed, purity 99.99% (GC). Carbon tetrachloride (Spectrum Chemical, ACS reagent) was distilled prior to use. All luminescence measurements were made on $1.06 \times 10^{-2}$ M benzophenone solutions in $CCl_4$. For phosphorescence/delayed fluorescence measurements, the solution was degassed using eight freeze−pump−thaw cycles to $4 \times 10^{-6}$ Torr and flame-sealed at a constriction. A 13 mm o.d. tube attached to a standard 1 $cm^2$ quartz cell via a sidearm and a graded seal was employed. Prompt fluorescence was measured for a $5.6 \times 10^{-3}$ M benzophenone solution in a standard 1 $cm^2$ quartz cell in the presence of air and 0.10 M *cis*-1,3-pentadiene (Aldrich, reagent). The *cis*-1,3-pentadiene was filtered through a short silica column immediately prior to use. The benzophenone solution used for absorption measurements was $0.93 \times 10^{-2}$ M in $CCl_4$.

**Spectroscopic Measurements.** All luminescence measurements were made with a Hitachi F-4500 fluorescence spectrophotometer equipped with a 150 W Xe arc source and a Hamamatsu R3788 photomultiplier tube. The scan rate was 60 nm/min, and slit widths were set at 5 nm for both excitation and emission monochromators. (The Hitachi F-4500 employs horizontal excitation and emission slits, instead of vertical ones as in our earlier work.[4]) Excitation wavelengths were 336 and 326 nm for DF/P and PF measurements, respectively. DF/P spectra were recorded in quintuplicate at 0.2 nm intervals in the 350−650 nm range for 16 different temperatures in the 14.7−88.5 °C range; see Table 1. Temperatures were maintained to within ±0.1 °C using a Neslab-RTE 4DD constant-temperature circulation bath. Temperatures were monitored continuously during each scan with an Omega Engineering model 199 RTD digital thermometer in a reference cell placed in the same constant-temperature cell holder. Forty spectra were recorded for PF at room temperature, ~22 °C. There was no change in the benzophenone absorption spectrum before and after the luminescence measurements. Absorption spectra were recorded for the temperatures used for the fluorescence measurements in the 14.7−68.1 °C range. A jacketed 1 cm path length cell

† On leave from the Faculty of Chemistry, Jagiellonian University, 30 060 Cracow, Poland.

10.1021/jp0200122 CCC: $22.00 
Published on Web 06/04/2002

**TABLE 1: Temperature Dependence of P and DF Contributions to Broadening-Compensated and Instrumental-Response-Corrected Benzophenone Spectra[a]**

| *T*, °C | $x_P$ | $x_{DF}$ | $10^2\phi_L$ | $10^{-5}k_{sq}$, $s^{-1}$ [c] | $10^{-2}k_FK$, $s^{-1}$ |
|---|---|---|---|---|---|
| 14.7 | 0.8328 (0.8296) | 0.1672 (0.1704) | 1.29 | 2.67 | 0.304 |
| 19.3 | 0.8087 (0.8063) | 0.1913 (0.1937) | 1.30 | 2.95 | 0.358 |
| 23.5 | 0.7845 (0.7829) | 0.2155 (0.2171) | 1.31[b] | 3.25 | 0.416 |
| 28.5 | 0.7536 (0.7530) | 0.2464 (0.2470) | 1.32 | 3.71 | 0.497 |
| 32.7 | 0.7295 (0.7295) | 0.2705 (0.2705) | 1.34 | 4.06 | 0.562 |
| 37.2 | 0.7046 (0.7052) | 0.2954 (0.2948) | 1.35 | 4.45 | 0.633 |
| 41.8 | 0.6790 (0.6809) | 0.3210 (0.3191) | 1.36 | 4.89 | 0.710 |
| 45.9 | 0.6539 (0.6562) | 0.3461 (0.3438) | 1.37 | 5.37 | 0.793 |
| 50.2 | 0.6325 (0.6354) | 0.3675 (0.3646) | 1.38 | 5.80 | 0.869 |
| 55.1 | 0.5991 (0.6030) | 0.4009 (0.3970) | 1.40 | 6.58 | 0.997 |
| 60.7 | 0.5646 (0.5696) | 0.4354 (0.4304) | 1.41 | 7.47 | 1.145 |
| 68.1 | 0.5197 (0.5261) | 0.4803 (0.4739) | 1.43 | 8.81 | 1.365 |
| 73.5 | 0.4910 (0.4985) | 0.5090 (0.5015) | 1.45 | 10.2 | 1.580 |
| 78.7 | 0.4604 (0.4688) | 0.5396 (0.5312) | 1.46 | 11.0 | 1.715 |
| 83.8 | 0.4299 (0.4394) | 0.5701 (0.5606) | 1.47 | 12.3 | 1.935 |
| 88.5 | 0.4018 (0.4124) | 0.5982 (0.5876) | 1.49 | 13.8 | 2.161 |

[a] Values in parentheses obtained from the spectrothermal matrix without correction for self-absorption. [b] Relative to this value taken from ref 2a after adjustment for the concentration-induced decrease in the triplet lifetime. [c] The benzophenone concentration was adjusted for the change in the density of $CCl_4$.

was used, and measurements were made with a Shimadzu UV-2100 spectrophotometer.

**Data Analysis.** The PCA-SM and singular value decomposition, SVD-SM, calculations were performed on a Dell Precision 530 1.4 GHz computer in the MATLAB 6.1 (release 12.1) environment using the Optimization Toolbox version 2.1.[6] Mathematical treatments were carried out on spectra that were not corrected for nonlinear instrumental response. However, the resolved spectra were corrected, and the fractional contributions that were used to derive the thermodynamic quantities were based on corrected spectra.

## Results

**Phosphorescence/Delayed Fluorescence Spectra.** A spectrothermal matrix of baseline-corrected benzophenone emission spectra under degassed conditions, Figure 1, was obtained by averaging the sets of 5 spectra for each of the 16 temperatures in Table 1. The onsets of the spectra in Figure 1 are corrected for self-absorption on the basis of the temperature dependence of the absorption spectrum of benzophenone, Figure 2, assuming a 0.5 cm effective path length. Because the measurements were made in a standard stoppered cell in the presence of air, the temperature range for the experimental absorption spectra was confined to 14.7−68.1 °C to avoid solvent loss. SVD-SM treatment of this partial set of absorption spectra showed it to be a two-component system and allowed (see the thermal sensitivity function approach below) derivation of extrapolated spectra for the higher temperatures. The eigenvectors and the temperature dependence of the major combination coefficient $\alpha$ that was used to extend the temperature range on the stoichiometric $\alpha,\beta$ line of the absorption spectra are available in the Supporting Information. The spectral matrix of self-absorption-corrected fluorescence spectra and the matrix of the original spectra without the correction for self-absorption were independently subjected to PCA-SM treatments. With or without the application of the self-absorption correction, PCA treatment reveals that the spectra are not represented cleanly as a two-component system. The relative magnitude of the third eigenvalue indicates a small but significant contribution from the third eigenvector, which was neglected in the earlier treatment of a similar data set.[4] Thermally induced shifts and broadening were considered as possible sources of this deviation from ideal two-component behavior. The possibility of systematic thermochromic shifts was tested by performing PCA treatments under the control of an algorithm which verifies whether a spectrum, potentially an outlier, requires shifting to achieve optimal match to a linear combination of the eigenspectra obtained from a selected reference set of the spectra confined to one of the extremes of the temperature range. This analysis predicted no shifts greater than 1 experimental point (0.2 nm), which is well within the experimental uncertainty of the measurements.

**Compensation for Broadening.** The procedure, developed recently for the resolution of a spectrothermal matrix composed of 1,3-butadiene vapor-phase absorption spectra,[6] was used to compensate for differential thermal broadening present in the benzophenone luminescence spectra. Ideally, this approach leads to a uniformly broadened spectral matrix corresponding to the highest experimental temperature. Since a detailed description of the preparation of the broadening-compensated spectral matrix is available,[6] a brief description of the method should suffice here.

The method employs convolution between each experimental spectrum and a corresponding derived effective thermal spread function to arrive at a new set of spectra, all possessing the thermal broadening present in the experimental spectrum for the highest temperature. The degree of broadening compensation is greatest for the experimental spectrum measured at the lowest temperature and becomes successively smaller as the experimental temperature of the spectrum is increased. The spectrum for the highest temperature is used as the reference spectrum and is entered in the modified matrix unchanged. The effective thermal spread functions are normalized Gaussian functions (unit area) with increasing heights and decreasing widths as corresponding temperatures approach the reference temperature (see the inset in Figure 1), such that convolution products between experimental spectra and corresponding spread functions preserve the integrated areas of the original spectra, differentially introducing only broadening in the shape of each spectrum. Derivation of the set of optimum spread functions for thermal broadening compensation requires identification of a single parameter, which corresponds to the width of the effective Gaussian spread function assigned to the lowest measured temperature. Gaussian spread functions corresponding to other temperatures are derived from this parameter on the basis of the expected dependence of thermal broadening on the temperature change. PCA treatments of the sets of thermally compensated spectra formed for each selected value of the broadening parameter (*k* in eq 9 of ref 6) are evaluated by tracing the evolution of the most significant eigenvalues. Specifically, the decrease of the relative magnitude of the third eigenvalue (ev3) with respect to the first (ev1) and second (ev2) can be used as the criterion for approaching a better two-component system. The location of minima in ev3/ev1 and ev3/ev2 vs *k* plots yields the optimum value of the *k* parameter, leading to the optimum set of thermally compensated spectra. As a second criterion, treatments of simulated two-component differentially broadened spectral matrices show that, on application of proper broadening compensation, oscillatory structural features in the derived second eigenvectors are suppressed.[6]

Nearly identical results were obtained for the uncorrected and the self-absorption-corrected luminescence spectra, and only the results for the latter are shown in the following figures. Application of the broadening compensation procedure to the spectra in Figure 1 is illustrated in Figures 3 and 4. Plots of ev3/ev1 and ev3/ev2 ratios vs the broadening parameter *k* show

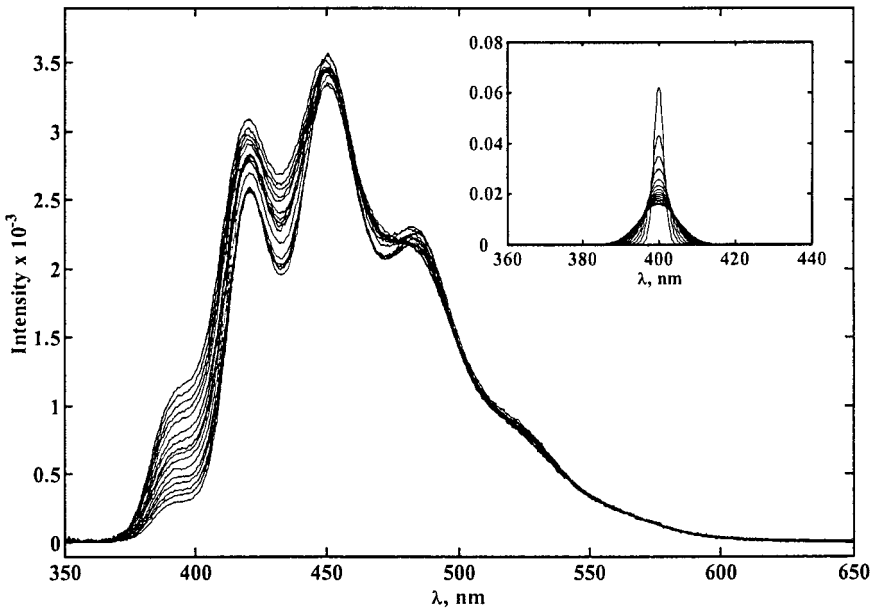


**Figure 1.** Benzophenone luminescence spectra (self-absorption-corrected, instrumental-response-uncorrected) at different temperatures (Table 1) from the degassed $CCl_4$ solution. The inset shows the set of Gaussian functions used to compensate the spectra for thermal broadening.

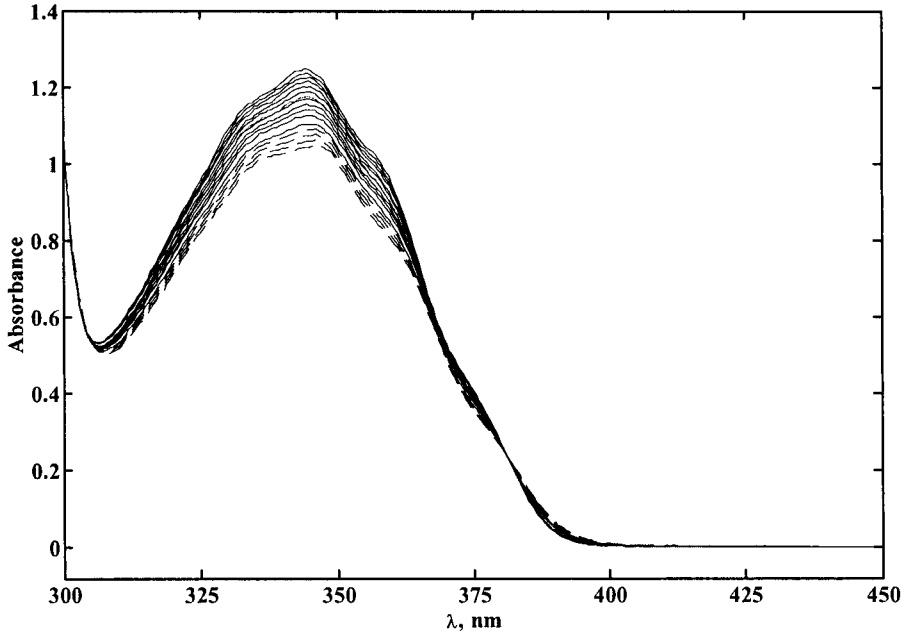


**Figure 2.** Temperature dependence of the n, $\pi^*$ absorption spectrum of a 0.0093 M benzophenone solution in $CCl_4$: experimental spectra (14.7−68.1 °C), solid lines; extrapolated spectra (73.5−88.5 °C), dashed lines (see the Supporting Information).

well-defined identical minima for $k = 3$ nm, Figure 3a. Convolution of the corresponding optimum set of spread functions (inset of Figure 1) with the spectra in Figure 1 leads to the broadening-compensated spectral set shown in Figure 4. Comparison of the two major eigenvectors before and after broadening, Figure 3b, reveals the expected pronounced attenuation of the oscillatory features in the second eigenvector on attaining more uniform broadening. No such dramatic changes are observed in the first eigenspectrum, which is somewhat broader due to the higher effective average temperature. The normalized compensated set of benzophenone emission spectra, Figure 4, shows a typical "pseudo"-isoemissive point at ca. 442 nm, characteristic of a normalized (unit area) two-component system.

**Resolution of the Compensated Spectral Matrix.** The PCA-SM method applied here to derive pure component spectra from the broadening-compensated benzophenone luminescence spectral matrices is identical to that applied earlier to a set of less well defined (1 point per 2 nm vs 1 point per 0.2 nm in this work) benzophenone spectra without compensation for broadening.[4,7] Rooted in the work of Lawton and Sylvestre (LS),[8] it modified the LS approach first by imposing a baseline at the onset and tail portions of the derived pure component trial spectra,[7] and later by introducing the van't Hoff constraint in SM.[4]

A set of two-component normalized emission spectra of benzophenone, $\mathbf{y}_{i,\mathrm{norm}}$, obeys the condition

$$\mathbf{y}_{i,\mathrm{norm}} = x_{i,\mathrm{P}}\mathbf{y}_{\mathrm{P,norm}} + x_{i,\mathrm{DF}}\mathbf{y}_{\mathrm{DF,norm}} \qquad (1)$$

where $\mathbf{y}_{\mathrm{P,norm}}$ and $\mathbf{y}_{\mathrm{DF,norm}}$ are the normalized pure P and DF spectra and $x_{i,\mathrm{P}}$ and $x_{i,\mathrm{DF}}$ are fractional contributions in the *i*th

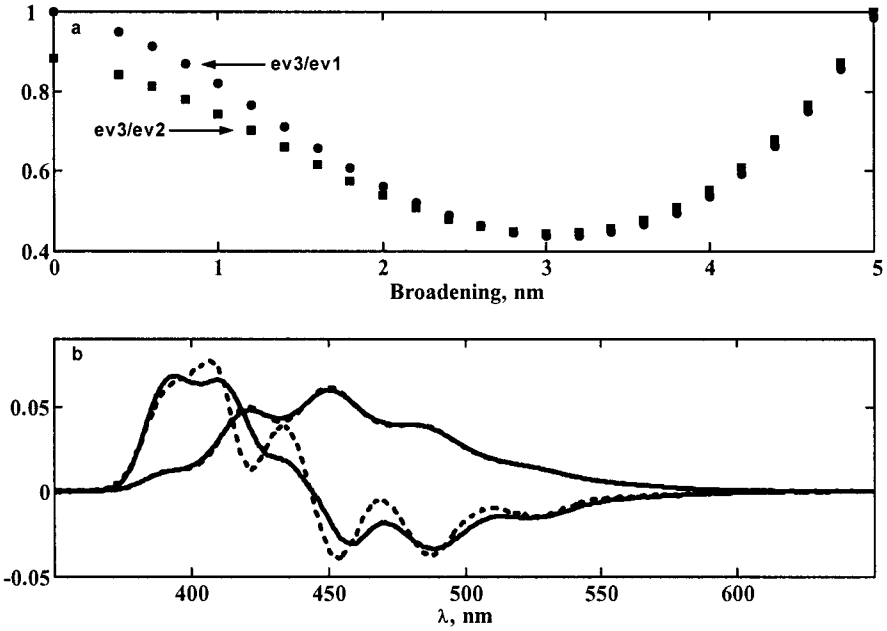


**Figure 3.** (a) Ratios of the third to the first eigenvalue (circles) and the third to the second eigenvalue (squares) as a function of the compensating broadening parameter *k*. (b) First and second eigenvectors before the compensation for thermal broadening (dashed lines) and after the compensation (solid lines).

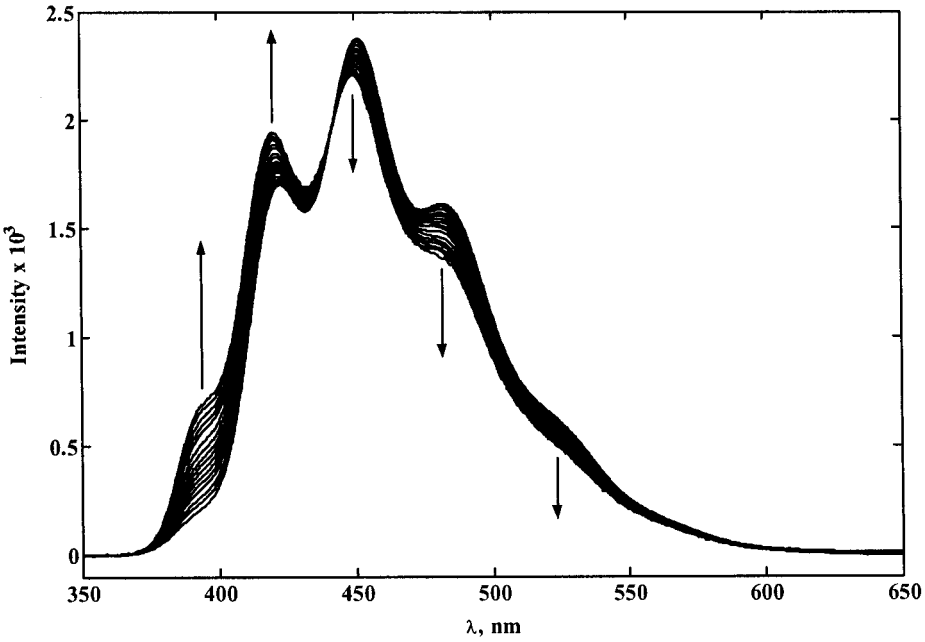


**Figure 4.** Benzophenone luminescence spectra in Figure 1 following broadening compensation and normalization to unit area.

spectrum. The PCA-SM method makes use of the fact that for a two-component system each experimental spectrum can also be effectively reconstructed as a linear combination of the first two eigenspectra (eigenvectors) $\mathbf{u}_\alpha$ and $\mathbf{u}_\beta$ provided by PCA

$$\mathbf{y}_{i,\text{norm}} = \alpha_i \mathbf{u}_\alpha + \beta_i \mathbf{u}_\beta \qquad (2)$$

where $\alpha_i$ and $\beta_i$ are the combination coefficients of the *i*th normalized experimental spectrum. The two principal eigenvectors define the normalization line in the $\alpha,\beta$ plane on which all combination coefficient pairs corresponding to the experimental spectra ($\alpha_i$, $\beta_i$) must fall. The combination coefficients for the compensated benzophenone luminescence spectra adhere very closely to the normalization line, Figure 5.

The combination coefficients of the pure component spectra are located on the normalization line outside the segment defined by the experimental spectra. Identification of the combination coefficients of the P spectrum on the normalization line was based on the previously established fact that only DF contributes at the onset region of the experimental spectra.[4,7] By systematically increasing the width of the onset region,[9] the desired pure DF onset range was shown to extend to 392 nm. The pure P spectrum was selected by imposing the best baseline to that region, Figure 6. The major difference between this P spectrum and that obtained previously[4,7] is that its vibronic structure is less well resolved because of the higher effective temperature (88.5 °C in this work vs $<-2.4$ °C in the earlier work). The slight oscillation at the onset was initially thought to be an artifact resulting from the temperature-dependent self-absorption of the DF at the onset region, less important in the earlier study because of the shorter path length (0.3 vs 1 cm cells) and the

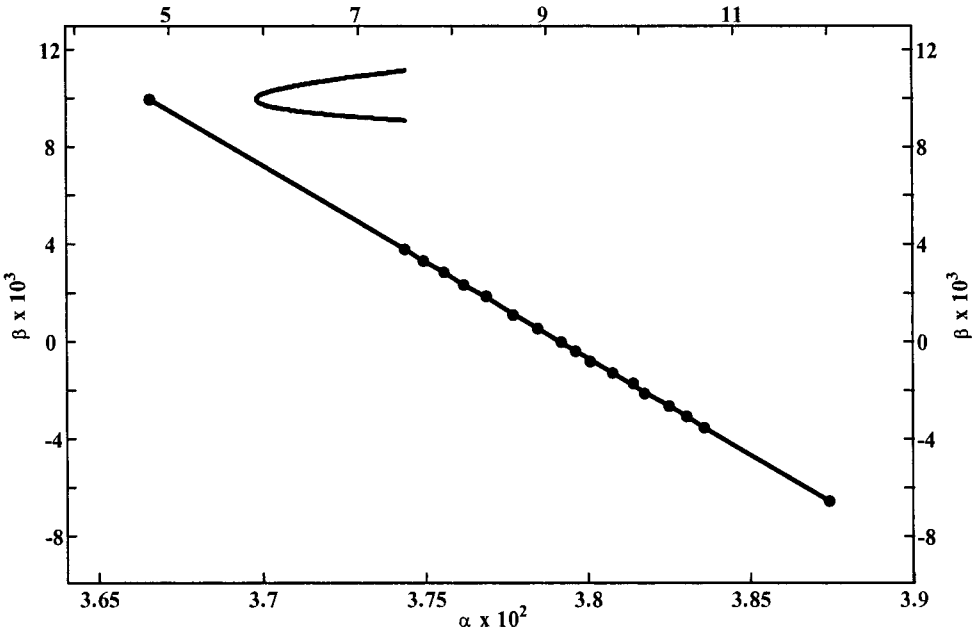


**Figure 5.** $\alpha,\beta$ normalization line for the benzophenone luminescence system. The standard deviation for the van't Hoff plot as a function of $\beta$ is also shown. The minimum determines the $\beta_{DF}$ value corresponding to the spectrum of the pure delayed benzophenone fluorescence.

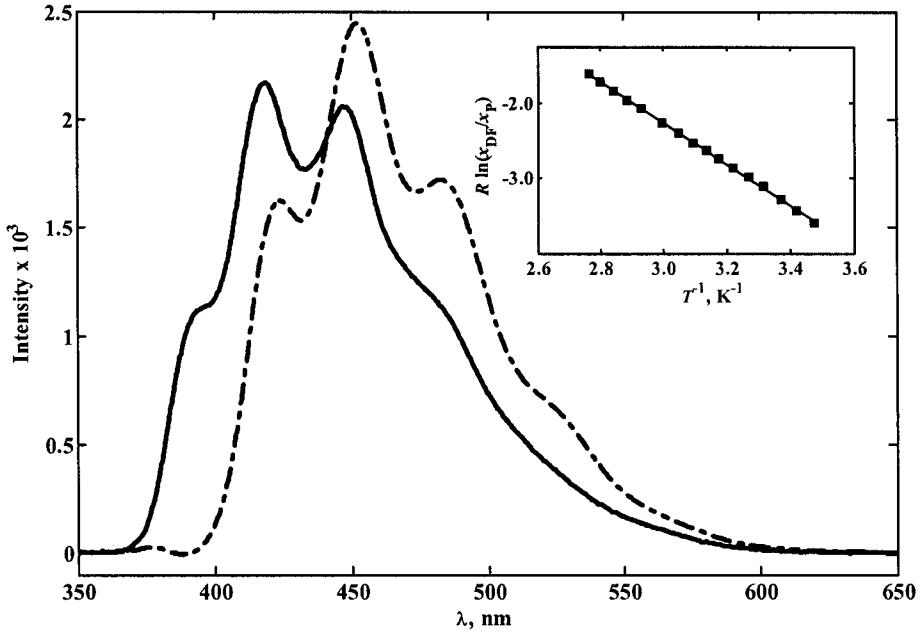


**Figure 6.** Broadening-compensated pure component P and DF spectra of benzophenone in $CCl_4$, $\lambda_{exc} = 336$ nm, 88.5 °C, uncorrected for nonlinearity in instrumental response and normalized to unit area. The inset shows a plot of the optimum van't Hoff plot for the equilibration of the $S_1$ and $T_1$ states of benzophenone obtained for the broadening-compensated experimental spectra corrected for nonlinearity in instrumental response.

10-fold smaller number of recorded intensities per nanometer. However, analyses before and after applying the corrections for self-absorption had little, if any, effect on this oscillation.

The search for the pure DF spectrum was based on the van't Hoff plot optimization constraint.[4,6] The thermodynamic equation that gives the temperature dependence of the fractional contributions of DF and P emissions from the equilibrated $S_1$ and $T_1$ states of benzophenone is

$$\ln(x_{i,DF}/x_{i,P}) = -(\Delta H/RT_i) + (\Delta S/R) + \ln(k_F/k_P) \quad (3)$$

where $k_{DF}$ and $k_P$ are the radiative rate constants for the $S_1 \rightarrow S_0$ and $T_1 \rightarrow S_0$ transitions (assumed temperature independent), respectively, and $\Delta H$ and $\Delta S$ are the enthalpy and entropy differences between the emitting states.[2a,4,7] A detailed description of the PCA-SM procedure with the use of the van't Hoff plot optimization constraint is available as an appendix in ref 6. The van't Hoff plot for the optimal $\beta_{DF}$ value is given as an inset in Figure 6. Both P and DF spectra, corrected for nonlinearity in instrumental response, are given in Figure 7. For the self-absorption-corrected spectral matrix, the value of the slope of the van't Hoff plot, based on fractional contributions corrected for instrumental response (Table 1), gives $\Delta H = 5.501 \pm 0.058$ kcal/mol (at the 95% confidence level), while the intercept yields $\Delta S/R + \ln(k_F/k_P) = 8.037 \pm 0.182$ (again at the 95% confidence level). The corresponding values for the self-absorption-uncorrected spectral matrix are $\Delta H = 5.331 \pm 0.052$ kcal/mol and $\Delta S/R + \ln(k_{DF}/k_P) = 7.765 \pm 0.164$.

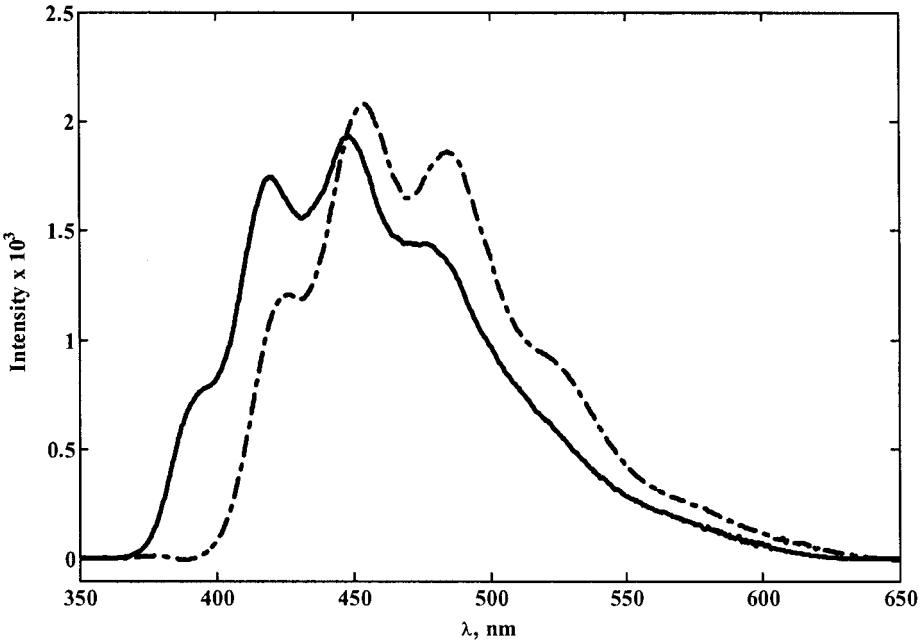


**Figure 7.** Broadening-compensated resolved emission spectra of benzophenone in $CCl_4$: P (dashed−dotted line) and DF (solid line) corrected for instrumental response and normalized to unit area.

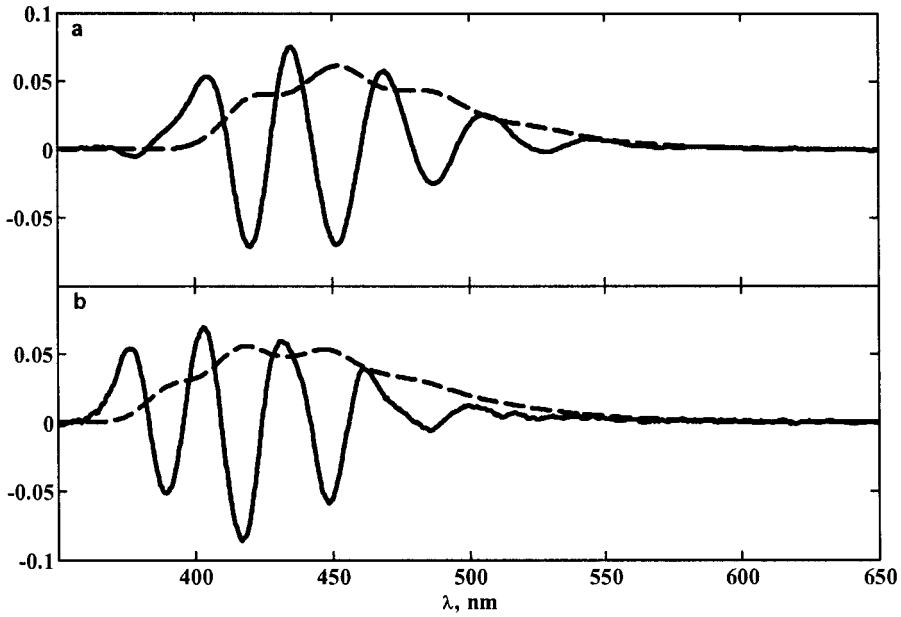


**Figure 8.** First (dashed line) and second (solid line) eigenvectors for the thermally broadened pure component spectra: (a) benzophenone phosphorescence and (b) delayed fluorescence. Pure component spectra uncorrected for instrumental response were used in constructing the matrices. The second eigenvectors are the thermal sensitivity functions that describe the change in the spectra of the individual components with temperature.

**Comparison of PF and DF Spectra.** To the degree that the thermal broadening compensation procedure succeeded in producing a uniformly broadened spectral matrix, corresponding to spectral mixtures at the highest experimental temperature, the P and DF pure component spectra shown in Figure 6 are those expected at 88.5 °C. Since the PF spectrum was measured at room temperature (22 °C), it is not proper to compare it directly with the derived DF spectrum. Either the PF spectrum must be convolved with the appropriate spread function to raise its temperature to 88.5 °C, or broadening must be removed from the DF spectrum in Figure 6 to convert it to the spectrum expected at ∼22 °C. Although less straightforward, the latter approach was undertaken because it was considered desirable to have pure component spectra at room temperature where most spectra are normally recorded, and because a method suited to this task was applied successfully in testing the agreement between the UV spectrum of jet-cooled *s-trans*-1,3-butadiene and the resolved spectrum of this conformer at 93 °C.[6] The procedure involves, as a first step, the creation of new spectrothermal matrices in which the derived high-temperature pure component spectra are projected to still higher temperatures by convolving them separately with the series of Gaussian spread functions in the inset of Figure 1. Since the number of spread functions and the temperature intervals are the same as before, the convolutions lead to a spectral matrix for each pure component in which the individual spectra are associated with the experimental $\Delta T$ values, and are modeled to possess the broadening expected for the 88.5−162.5 °C $T$ range. As expected, PCA treatment of these derived spectrothermal matrices shows them to behave as two-component systems

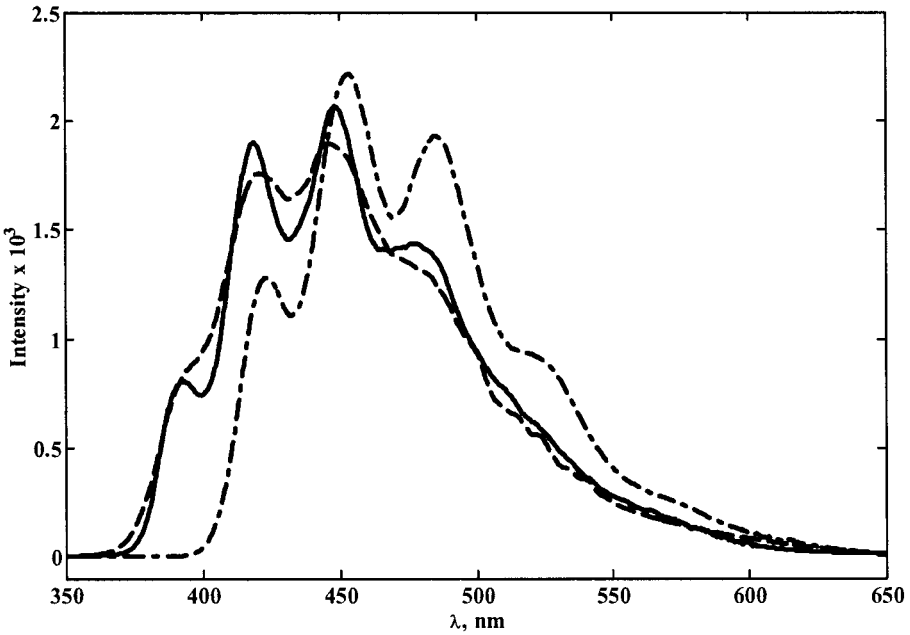


**Figure 9.** Emission spectra of benzophenone in $CCl_4$ corrected for nonlinearity in instrumental response and normalized to unit area: phosphorescence (dashed−dotted line), delayed fluorescence (solid line), and prompt fluorescence (dashed line). The first two spectra are obtained by extrapolation of the $\alpha$, $\beta$ coefficients of the pure component spectra to 23.5 °C, and the prompt fluorescence is an average of 40 spectra measured at room temperature (ca. 22.0 °C) for $\lambda_{exc} = 326$ nm.

where the first eigenspectra are the average of the spectra in the two matrices and the second eigenspectra are the thermal sensitivity functions of P and DF, respectively, Figure 8.[4,10−12] The temperature dependence of the $\alpha$ and $\beta$ coefficients allows their extrapolation to lower temperatures. In this instance, the dependence of the $\alpha$ coefficients on $T$ appears to be linear, while the plot of the $\beta$ coefficients vs $T$ shows slight curvature. Extrapolation of the two sets of $\alpha$ and $\beta$ coefficients to 23.5 °C followed by a slight smoothing of the baseline regions and correction for nonlinearity in instrumental response leads to the predicted spectra in Figure 9. Also shown in Figure 9 is the instrumental-response- and self-absorption-corrected average of the 40 PF spectra.

## Discussion

Aartsma and co-workers reported the first PCA-SM-based resolution of a spectrothermal luminescence matrix.[13] With the use of LS nonnegativity criteria a matrix of platinum tetrabenzoporphyrin phosphorescence spectra measured at different temperatures was resolved into pure component spectra from two equilibrating triplet sublevels. The same procedure was applied in this laboratory to the initial resolution of benzophenone luminescence spectra, obtained under experimental conditions similar to those described in this paper, into P and DF spectra,[7] and later the choice of the DF spectrum was refined by the use of the van't Hoff plot optimization constraint.[4] Although seemingly successful, those PCA-SM resolutions neglect the influence of differential thermal broadening, present in the experimental spectra, on the shape of the derived pure P and DF spectra. Our initial resolution of a spectrothermal matrix of gas-phase 1,3-butadiene UV spectra into *s-trans*- and *s-cis*-1,3-butadiene conformer spectra similarly neglected the effect of temperature-dependent broadening on the derived spectra.[14]

The profound effect of broadening on such PCA-SM resolutions was demonstrated with the use of simulated matrices of differentially broadened two-component spectra.[6] It was found that broadening affects PCA-SM results by causing significant departure from two-component behavior and pronounced distortion in the shape of the second eigenvector, which are reflected in the shapes of the derived pure component spectra.[4] Recovery of the correct pure component spectra from simulated spectral matrices was achieved through a broadening compensation procedure that converts the differentially broadened matrix to a uniformly broadened matrix.[6] The broadening compensation procedure was applied to the resolution of the 1,3-butadiene UV absorption spectra[6] and is applied here to the resolution of the benzophenone luminescence spectra. We were motivated in this work, at least in part, by the desire to evaluate the conclusion that DF and PF benzophenone emissions differ significantly.

**P/DF Spectra.** The effect of using the broadening-compensated spectral matrix in the PCA-SM treatment on the spectral resolution is readily appreciated by comparing our spectra in Figure 6 with those in Figure 2 of ref 7. The comparison is valid because both sets of spectra are uncorrected for instrumental response and, although different spectrophotometers were employed in the two studies, we have established that the correction factors for the two instruments are nearly identical. Immediately evident is the fact that broadening compensation affects the derived P and DF resolved spectra in the opposite way. Compensation leads to better resolution in the vibronic structure of the DF spectrum and lower resolution in the P spectrum, in large part due to the differences in the effective temperatures of the resolved spectra. Whereas both spectra in Figure 6 are for 88.5 °C, the highest experimental temperature used in this work, in ref 7 the P spectrum corresponds to a temperature lower than −2.4 °C and the DF spectrum corresponds to a temperature higher than 85.2 °C, the lowest and highest temperatures used in the earlier study. This is because movement on the normalization line away from the segment defined by the uncompensated experimental spectra extends the temperature of derived spectra to lower and higher values in addition to changing the P/DF composition. Projection of the P and DF spectra in Figure 6 to 23.5 °C, as described in the Results, leads to higher resolution of vibronic structure in both spectra, Figure 9.

The discrepancy between the tail regions of the DF spectra in Figure 6 and in ref 7 is due, in part, to the application of broadening compensation in the present study and, in part, to the fact that the earlier spectrum is an outer limit spectrum on the basis of the LS nonnegativity constraint, whereas the spectrum in Figure 4 is uniquely defined by the van't Hoff plot optimization constraint. No well-defined minimum in the standard deviation of the van't Hoff plot could be found earlier,[4] without the application of the broadening compensation procedure. The present PCA-SM approach provides a quantitative analysis of the experimental spectral system of benzophenone luminescence in terms of P and DF spectral contributions, Table 1. Nearly identical fractional compositions are derived by application of the self-absorption correction on the experimental spectra prior to PCA-SM treatment, or on the resolved spectra following PCA-SM treatment of the uncorrected spectra.

**Thermodynamic Parameters for $T_1/S_1$ Equilibration.** The temperature dependence of the fractional contributions of P and DF, based on the somewhat arbitrarily selected pure component DF spectrum, had yielded $\Delta H = 6.3 \pm 0.3$ kcal/mol and $\Delta S = 0.7 \pm 1.0$ eu for the $T^1$ to $S^1$ direction.[4] In contrast, application of the van't Hoff optimization procedure on the broadening-compensated benzophenone luminescence spectra is straightforward, leading to unambiguous selection of the combination coefficients of the DF spectrum, Figure 5. The optimum van't Hoff plots of the two sets of fractional contributions in Table 1 give substantially different values. The plot based on the PCA-SM treatment of the self-absorption-corrected spectra (inset in Figure 6) gives $\Delta H = 5.50 \pm 0.06$ kcal/mol and $\Delta S = -1.59 \pm 0.18$ eu, whereas the plot based on the treatment of the unaltered experimental spectra gives $\Delta H = 5.33 \pm 0.05$ kcal/mol and $\Delta S = -2.14 \pm 0.16$ eu. The near identity of the new $\Delta S$ values with $-R \ln 3 = -2.18$ eu, the value expected if $\Delta S$ reflected solely the statistics of the multiplicity change, seems much more than coincidental and is an excellent validation of our broadening compensation method. It eliminates the need[4] to postulate significant differences in conformational freedom between two n,$\pi^*$ states that differ in multiplicity but have identical orbital occupancies. The small deviation between the two new $\Delta S$ values is not considered significant as these values depend on the accuracy of the ratio of radiative rate constants used in their derivation, eq 3. We used $k_F = 1.1 \times 10^6$ s$^{-1}$ and $k_P = 1.6 \times 10^2$ s$^{-1}$ as before,[4] although it can be argued that $k_F = 1.2 \times 10^6$ s$^{-1}$ and $k_P = 1.4 \times 10^2$ s$^{-1}$ or smaller are preferable values.[4] Use of the latter set of radiative rate constants would lead to adjustment of the larger $\Delta S$ value from $-1.58 \pm 0.18$ to $-2.02 \pm 0.18$ eu, well within experimental uncertainty of $-R \ln 3$.

Regarding the $\Delta H$ value, we were content in the earlier study with the fact that a 6.3 kcal/mol $S^1-T^1$ energy splitting, based on estimated 0−0 bands in the $S^1 \leftarrow S^0$ absorption and the $T^1 \leftarrow S^0$ phosphorescence excitation spectra of benzophenone in a 2:1:1 ether/ethanol/toluene glass at 77 K,[15] was identical to the derived value.[4] The much more reliable ~1.0 kcal/mol lower values obtained in this work suggest significant solvent and temperature effects on this quantity and encourage us to rely on our spectra for the spectroscopic estimation of this energy gap. Since the emission spectra in Figure 9 are composed of strongly overlapping broad vibronic bands, their 0−0 bands are not clearly defined. Better definition of the energies of these bands was achieved by fitting several Gaussian envelopes to each spectrum, Table 2. The first Gaussian envelopes in the resolved DF and P spectra, taken as defining the relative positions of the 0−0 bands, give 5.42 kcal/mol from the self-absorption-corrected spectral matrix and 5.34 kcal/mol when the self-absorption correction is deferred to the end of the PCA-SM treatment, in excellent agreement with values of $\Delta H = 5.53 \pm 0.06$ and $5.33 \pm 0.05$ kcal/mol from the slopes of the corresponding van't Hoff plots. Application of the Gaussian fitting procedure to the PF spectrum in Figure 9 generates a set of five Gaussians, the first three of which are centered at wavelengths nearly identical (to within ±0.3 nm) with those for the DF spectrum.

**TABLE 2: First Three Vibronic Bands in the Emission Spectra Based on Gaussian Fitting[a]**

| vibronic band max | P, 88.5 °C | DF, 88.5 °C | P, 23.5 °C | DF, 23.5 °C | PF, 22 °C |
|---|---|---|---|---|---|
| first | 422.2 (422.0) | 390.9 (391.1) | 421.9 | 391.3 | 391.4 |
| second | 451.4 (451.6) | 418.6 (418.4) | 451.6 | 418.3 | 418.0 |
| third | 484.3 (485.0) | 446.4 (446.2) | 485.0 | 446.5 | 446.4 |

[a] Band maxima in nanometers; for spectra corrected for nonlinearity of instrumental response and for self-absorption. Values in parentheses are for pure component spectra corrected for self-absorption after their derivation from the analysis of self-absorption-uncorrected spectra.

The positions of the true 0−0 bands would be defined better from the overlap of corresponding absorption and emission transitions. A similar Gaussian fitting performed for the benzophenone $S^1 \leftarrow S^0$ absorption spectrum, Figure 2, locates the position of the maximum of the first Gaussian envelope at 376.3 nm, substantially to the blue of the corresponding peak in the fluorescence spectra. The average of the positions of the first peaks in absorption and fluorescence spectra, 384.0 nm, gives a crude estimation of the true position of the 0−0 gap in the $S^1-S^0$ electronic transition, corresponding to an energy of 74.5 kcal/mol.

**Temperature Effect on Luminescence Quantum Yields.** The increase in the contribution of DF with increasing temperature is reflected in a monotonic increase in the area of the spectra (corrected for nonlinearity in instrumental response) in Figure 1. The luminescence quantum yield, $\phi_L = 1.5 \times 10^{-2}$, obtained at 23 °C for a $5 \times 10^{-3}$ M benzophenone solution in $CCl_4$,[2a] was adjusted downward to $1.31 \times 10^{-2}$ to account for increased self-quenching[16] at the higher concentration employed in this work. This value was used to convert the relative areas of the luminescence spectra to quantum yields (Table 1) after a small correction for the temperature dependence of the absorbance at 336 nm was applied, Figure 2. The increase of the luminescence quantum yield of about 16% over our temperature range can be compared with the somewhat larger increase of 36% observed earlier for a larger temperature range.[4] The difference between the two sets of data is well within the experimental uncertainty of the measurements. Our new measurements strengthen the conclusion that the increase in $\phi_L$ is considerably smaller than the nearly 2-fold increase that should accompany the enhanced singlet-excited-state equilibrium population, provided that the radiative rate constants and the benzophenone triplet lifetime were temperature independent.

The estimated 13% decrease in the area of the n, $\pi^*$ absorption band in Figure 2 is accounted for, nearly exactly, by a corresponding change of 10% in the density of the solvent,[17] indicating that $k_F$ is not sensitive to the temperature. Since $k_P$ should be similarly temperature independent, the increase in $\phi_L$ is moderated by a significant decrease in the triplet lifetime with increasing temperature. The luminescence decay rate, $k_d$, of benzophenone triplets in degassed $CCl_4$ at ambient temperature depends on the benzophenone concentration, [B],

due to self-quenching in which hydrogen abstraction plays a small role[16]

$$k_d = k_d^0 + k_{sq}[B] \quad (4)$$

where the extrapolated value of $k_d^0 = 1.13 \times 10^4\ s^{-1}$ agrees well with the decay rate constant ($1.06 \times 10^4\ s^{-1}$) reported earlier for a relatively dilute benzophenone solution,[18] and $k_{sq} = 3.25 \times 10^5\ M^{-1}\ s^{-1}$.[16] Since PF contributes negligibly to the $\phi_L$ values in Table 1, we can write

$$\phi_L = f_S k_F \tau_T + f_T k_P \tau_T \quad (5)$$

where the sum of the fractions of molecules in the singlet and triplet excited states $f_S + f_T = 1$ and $\tau_T = k_d^{-1}$. Assuming that the pseudo-unimolecular rate constant $k_d^0$ is temperature independent, we tentatively attribute part of the variation of $\phi_L$ with temperature on the temperature dependence of $k_{sq}$. Multiplication of the $\phi_L$ values by the fractional contributions in Table 1 yields $\phi_{DF}$ and $\phi_P$ values. In view of the very small $[S_1]/[T_1]$ equilibrium constants, $K$, throughout our temperature range, $f_S = K$, $f_T = 1$, and the two terms in eq 5 can be written as $\phi_{DF} = Kk_F\tau_T$ and $\phi_P = k_P\tau_T$. Use of $k_d = 1.47 \times 10^4\ s^{-1}$ at 23.5 °C for [B] = 1.06 M[16] gives $k_P = 1.52 \times 10^2\ s^{-1}$, well within the range of experimental values (see above). The temperature dependence of $k_d$ can now be estimated from $k_P/\phi_P$, and its variation can be attributed to $k_{sq}$ by subtraction of $k_d^0$. The Arrhenius plot of the resulting $k_{sq}$ values (fifth column of Table 1) gives an activation energy of 4.6 kcal/mol and a rather low preexponential factor of $7.76 \times 10^8\ M^{-1}\ s^{-1}$. The analysis was tested for internal consistency by calculating $Kk_F$ values at the experimental $T$ values from the $k_d\phi_{DF}$ products, Table 1. The plot of $\ln Kk_F$ vs $T^{-1}$ is strictly linear ($r = -0.9996$), and gives $\Delta H = 5.40 \pm 0.04$ kcal/mol and, assuming $\Delta S = -2.18$ eu, $k_F = (1.17 \pm 0.08) \times 10^6\ s^{-1}$, in excellent agreement with the values obtained above from the van't Hoff treatment of the fractional contributions.

**Comparison of DF and PF Spectra.** A primary motivation for this work was to determine whether the conclusion that DF and PF spectra are significantly different was due to distortions in the resolved DF spectrum as a consequence of having neglected the effect of differential thermal broadening on the PCA-SM treatment.[4] The more reliable DF and PF spectra obtained in this work are compared at about the same temperature in Figure 9. The near coincidence of the positions of the vibronic bands that was determined by the Gaussian fitting procedure (Table 2) is evident qualitatively at a glance, and the conclusion that PF and DF spectra are not identical is confirmed. The PF spectrum is significantly more diffuse than the DF spectrum, consistent with emission contributions from vibrationally hot $S_1$ states. Complete vibrational relaxation is not attained within the 10 ps lifetime[5] of the $S_1$ state of benzophenone.

**Acknowledgment.** NSF Grant CHE 9985895 supported this research. We thank Professor Igor Alabugin for the use of the Shimadzu UV-2100 spectrophotometer.

**Supporting Information Available:** Figure S1, the eigenvectors, and Figures S2 and S3, the temperature dependence of the combination coefficients, used in extending the temperature range of the benzophenone absorption spectra. This material is available free of charge via the Internet at http://pubs.acs.org.

## References and Notes

(1) (a) Borisevich, N. A.; Gruzinskii, V. V. *Dokl. Akad. Nauk. SSSR* **1967**, *175*, 852. Cf. also: (b) Dorokhin, A. V.; Kotov, A. A. *Opt. Spectrosc. (USSR)* **1981**, *51*, 617.

(2) (a) Saltiel, J.; Curtis, H. C.; Metts, L.; Miley, J. W.; Winterle, J.; Wrighton, M. *J. Am. Chem. Soc.* **1970**, *92*, 410−411. (b) Brown, R. E.; Singer, L. A.; Parks, J. H. *Chem. Phys. Lett.* **1972**, *14*, 193. (c) Brown, R. E.; Legg, K. D.; Wolf, M. W.; Singer, L. A.; Parks, J. H. *Anal. Chem.* **1974**, *46*, 1690. (d) Wolf, M. W.; Legg, K. D.; Brown, R. E.; Singer, L. A.; Parks, J. H. *J. Am. Chem. Soc.* **1975**, *97*, 4490.

(3) (a) Jones, P. F.; Calloway, A. R. *J. Am. Chem. Soc.* **1970**, *92*, 4997. (b) Jones, P. F.; Calloway, A. R. *Chem. Phys. Lett.* **1971**, *10*, 438.

(4) Sun, Y.-P.; Sears, D. F., Jr.; Saltiel, J. *J. Am. Chem. Soc.* **1989**, *111*, 706−711.

(5) Greene, B. I.; Hochstrasser, R. M.; Weisman, R. B. *J. Chem. Phys.* **1979**, *70*, 1247.

(6) Saltiel, J.; Sears, D. F., Jr.; Turek, A. M. *J. Phys. Chem. A* **2001**, *105*, 7569−7578.

(7) Sun, Y.-P.; Sears, D. F., Jr.; Saltiel, J. *Anal. Chem.* **1987**, *59*, 2515−2519.

(8) (a) Lawton, W. H.; Sylvestre, E. A. *Technometrics* **1971**, *13*, 617−633. (b) Sylvestre, E. A.; Lawton, W. H.; Maggio, M. S. *Technometrics* **1974**, *16*, 353−368.

(9) Saltiel, J.; Sears, D. F., Jr.; Sun, Y.-P.; Choi, J.-O. *J. Am. Chem. Soc.* **1992**, *114*, 3607−3612.

(10) Saltiel, J.; Choi, J.-O.; Sears, D. F., Jr.; Eaker, D. W.; Mallory, F. B.; Mallory, C. W. *J. Phys. Chem. A* **1994**, *98*, 13162−13170.

(11) Nodland, E.; Libnau, F. O.; Kvalheim, O. M.; Luinge, H.-J.; Klaeboe, P. *Vib. Spectrosc.* **1996**, *10*, 105−123.

(12) Nodland, E.; Libnau, F. O.; Kvalheim, O. M. *Vib. Spectrosc.* **1996**, *12*, 163−176.

(13) Aartsma, T. J.; Gouterman, M.; Jochum, C.; Kwiram, A. L., Pepich, B. V.; Williams, L. D. *J. Am. Chem. Soc.* **1982**, *104*, 6278−6283.

(14) Sun, Y.-P.; Sears, D. F., Jr.; Saltiel, J. *J. Am. Chem. Soc.* **1988**, *110*, 6277−6278.

(15) (a) Kearns, D. R.; Case, W. A. *J. Am. Chem. Soc.* **1966**, *88*, 5087−5097. (b) Borkman, R. F.; Kearns, D. R. *J. Chem. Phys.* **1967**, *46*, 2333.

(16) Schuster, D. I.; Weil, T. M. *Mol. Photochem.* **1974**, *6*, 69−80.

(17) Timmermans, J. *Physico-Chemical Constants of Pure Organic Compounds*; Elsevier: New York, 1950; Vol. I.

(18) Merkel, P. B.; Kearns, D. R. *J. Chem. Phys.* **1973**, *58*, 398.